J Polym Res (2015) 22: 189
DOI 10.1007/s10965-015-0828-x

ORIGINAL PAPER

Synthesis, microstructural characterization and hydrophobic intermolecular nano-aggregation behavior of acrylamide/2-acrylamido-2-methy-1-propane sulfonic acid/butyl acrylate co- and terpolymers

Hossein Khakpour[1] · **Mahdi Abdollahi**[1] · **Alireza Nasiri**[2]

Received: 25 April 2015 / Accepted: 24 August 2015 / Published online: 8 September 2015
© Springer Science+Business Media Dordrecht 2015

Abstract Acrylamide(AM)/butyl acrylate (BA) (as a hydrophobic monomer) copolymers and an AM/BA/2-acrylamido-2-methy-1-propane sulfonic acid (AMPS) terpolymer were synthesized in an aqueous medium using potassium persulfate as an initiator, in which heterogeneous (without emulsifier) and micellar (in the presence of sodium dodecyl sulfate as an emulsifier) copolymerization methods were employed. Fourier transform infrared (FTIR) and nuclear magnetic resonance (NMR) spectroscopy techniques were used to characterize the synthesized co- and terpolymers. Copolymer composition was determined from ^{1}H-NMR spectra. The microstructure of the AM/BA copolymers was also evaluated through measurement of water solubility and calculation of the hydrophobic block length and monomer sequence length. The molecular weight of the copolymers was calculated from intrinsic viscosity measurements to be in a range of (0.5–1.5)×10^{6} g/mol. Results showed that the heterogeneous and micellar copolymerization methods resulted in random and multi-block distribution, respectively, of the BA comonomer in the copolymer chains. A reasonable relationship between the microstructure and water solubility of the copolymers was established. A hydrophobic BA block length (i.e., number of BA units per micelle) of approximately 10 was obtained using the micellar copolymerization method, which was found to be a limiting factor with regard to the water solubility of the copolymers. Dynamic light scattering measurements were used to study the hydrodynamic radii and hydrophobic nano-aggregation behavior of the samples. The hydrodynamic radii of polymer chains in a dilute aqueous solution were found to be in a range of 1–36 nm. Due to the presence of BA-associating hydrophobic groups, a small fraction of aggregations larger than 100 nm were also observed.

Keyword Hydrophobically modified polyacrylamide · Acrylamide/Bbutyl acrylate · Micellar copolymerization · Copolymer microstructure · Water solubility · Hydrophobic intermolecular nano-aggregates

Introduction

Because of its high molecular weight, polyacrylamide (PAM) has found wide use as a thickening agent and rheology modifier in a variety of applications across a number of industries. However, the rheological properties of polyacrylamides are reduced at high temperatures and in the presence of high salt concentrations [1–5]. In a number of studies, certain hydrophilic monomers such as 2-acrylamido-2-methyl-1-propane sulfonic acid (AMPS) have been observed to improve the rheological properties and thermal stability of acrylamide (AM)-based copolymers [6–10]. Thus, AM-based copolymers have been synthesized to improve rates of shear resistance, salt resistance and thermal stability [1–6, 11–13]. By incorporating the hydrophobic comonomer as a modifier into the PAM main chain, hydrophobically modified polyacrylamide (HMPAM) can be synthesized [1–6, 14–26]. HMPAMs are one of the most important polymers used as rheology modifiers, and have found many applications in the enhanced oil recovery and drilling muds, dyes and detergent products [1–6, 11–20]. These desirable thickening and rheology

✉ Mahdi Abdollahi
abdollahim@modares.ac.ir

[1] Polymer Reaction Engineering Department, Faculty of Chemical Engineering, Tarbiat Modarres University, P.O. Box: 14115-114, Tehran, Iran

[2] Petroleum Engineering Division, Research Institute of Petroleum Industry, P.O. Box: 14665-1998, Tehran, Iran

modification properties are attributed to the HMPAMs' microstructure [1–6]. Hydrophobic comonomers commonly used in HMPAM synthesis include *n*-alkyl acrylates and acrylamides [1–6, 11–16]. The improved rheological properties in HMPAMs are induced through the formation of associations and physical networks of hydrophobic groups.

Researchers investigating the copolymerization of AM with a small amount of fluorinated (meth)acrylate for the synthesis of HMPAM reported associative behavior among the hydrophobic groups [27]. Another work demonstrated strong pseudo-plastic behavior of prepared samples using rheology tests in which viscosity measurements were carried out under various conditions by increasing temperature, salt concentration and cosolvent content [27]. The preparation of hydrophobically modified polyelectrolytes from acrylic acid and 3-[Tris(trimethylsiloxy)silyl]propyl methacrylate has been reported in the literature [28], where structural characterization and rheological properties were studied using FTIR, ^{1}H-NMR, TEM and viscometry techniques. PH dependence of the viscosity has been observed with a maxima at around pH=5.5 [28].

The synthesis of acrylic acid/alkyl acrylate (alkyl chain with lengths of 8, 12, 14, 16 or 18) via solution polymerization and a random distribution of alkyl acrylate in the copolymer chain has been reported [29]. These copolymers exhibited strong associative behavior in the aqueous medium, and consequently, the intrinsic viscosity measurements of prepared samples demonstrated intra-chain association in the dilute solutions. Viscosity has been found to depend on copolymer concentration, temperature, shear rate, ionic strength and pH [29].

Despite its wide accessibility, low cost and hydrophobicity, the BA monomer has never been considered regarding its potential applicability for the synthesis of HMPAMs. Thus, in the present work, we investigated the heterogeneous and micellar copolymerization of AM and BA in the synthesis of water-soluble hydrophobically associating copolymers. It should be mentioned that radical solution (homogeneous) and microemulsion copolymerization of AM and BA has been reported [30–34]. In a study involving nitroxide-mediated controlled radical polymerization of *N*,*N*-dimethyl acrylamide, followed by BA in dimethylformamide (DMF) as a solvent, by following reaction kinetics, a narrow molecular weight distribution with a polydispersity index (PDI) of about 1.08 was obtained for the corresponding diblock copolymer [30]. Copolymerization of AM and BA through microemulsion has also been studied, and the reaction kinetics, conversion and copolymer composition have been reported [31]. In one work in which free radical solution copolymerization of AM and alkyl acrylates (ethyl and butyl acrylate) was initiated with benzoyl peroxide at 65 °C in DMF as solvent, the sequence distribution of the monomer was investigated using an NMR technique. The reactivity ratios of AM and BA in the DMF solution, calculated using the Kelen-Tüdös method, were found to be 0.69 and 1.24, respectively [32]. Therefore, this free radical copolymerization was shown to proceed via random copolymerization [32].

Molecular weight, copolymer composition and distribution of the hydrophobic comonomer in the copolymer chain are key microstructure-related parameters with significant effects on the rheological properties and associative behavior of hydrophobic groups [2]. Static light scattering (SLS) and intrinsic viscosity are two techniques commonly used to determine the molecular weight of HMPAMs [2–6, 15–17] .^{1}H-NMR and ultraviolet (UV) spectroscopy techniques can be used for determining copolymer composition. Depending on the copolymerization technique, a random or multi-block distribution of the hydrophobic monomer in the main chain would be expected, resulting in random or multi-block copolymers, respectively. Thus, the final desired microstructure of HMPAM can be designed by employing an appropriate polymerization technique [1–4].

Various polymerization techniques can be used for the synthesis of HMPAMs, including heterogeneous, homogeneous and micellar copolymerization. Homogeneous polymerization requires the dissolution of the comonomer in a cosolvent, whereby the hydrophilic main monomer and hydrophobic comonomer are copolymerized in an aqueous phase in the presence of a cosolvent. In contrast, copolymerization of the hydrophilic and hydrophobic monomers in heterogeneous polymerization needs no such cosolvent addition. By employing heterogeneous or homogeneous polymerization, the BA hydrophobic comonomer would be distributed randomly in the copolymer main chain [1–5]. In micellar polymerization, however, micelles are formed due to the use of emulsifiers. Micelles provide favorable sites for the dissolution and association of hydrophobic monomers. Therefore, hydrophobic blocks of different lengths can be formed upon penetration of free radicals into the micelles, which then enter the main chain and form a multi-block microstructure [1–5, 12, 13].

As mentioned above, the copolymerization of AM and BA has been reported [30–34], but previous studies were not designed to prepare HMPAMs or study their physical properties in aqueous solutions. In the present work, HMPAMs based on AM/BA copolymers and an AM/AMPS/BA terpolymer were synthesized for the first time via micellar co- and terpolymerization methods in the presence of a sodium dodecyl sulfate (SDS) emulsifier. AM and BA were used as the main hydrophilic monomer and the hydrophobic comonomer, respectively. To investigate ionic comonomer effects, AMPS was also used as a hydrophilic comonomer [35]. The chemical structure of the prepared samples was characterized using FTIR and ^{1}H-NMR and ^{13}C-NMR techniques. ^{1}H-NMR was also used to experimentally measure the composition and conversion of the synthesized HMPAMs. Theoretical

equations and ^{1}H-NMR spectra were used for evaluation of the samples' microstructure. A water solubility test was then used to determine the relationship between the solubility and microstructure of the synthesized polymers. Molecular weight was determined using intrinsic viscosity measurements. The hydrophobic aggregation behavior and hydrodynamic radius (R_h) of the samples were also studied by measuring water solubility, intrinsic viscosity and dynamic light scattering (DLS).

Experimental

Materials

The AM used for synthesis was purchased from Merck, Millipore, and was recrystallized twice in acetone. The BA, also purchased from Merck, was purified by passing it through a basic alumina column. Potassium persulfate (KPS) and AMPS, both from Merck, were used without further purification. NaCl (purity>99 %), acetone (purity>99 %) and methanol were purchased from Dr. Mojallali Chemical Complex Co. (Tehran, Iran). SDS (99.9 % purity) from Daejung Chemical and Metals Co., Ltd. (Siheung-si, Korea) was used as received. Deionized water and nitrogen (purity>99.9 %) were used in all experiments.

Copolymer and terpolymer synthesis

The micellar copolymerization method was used for the synthesis of the AM/BA copolymers and AM/AMPS/BA terpolymer, with SDS and KPS were employed as emulsifier and initiator, respectively. Only one copolymer from AM/BA was also synthesized heterogeneous copolymerization. A 50-ml ampoule containing 40 ml distilled water, as aqueous phase, was used as a reaction chamber. With the use of a magnetic stirrer over a period of 30 min, predefined amounts (Table 1) of AM (as well as AMPS for the terpolymer synthesis), BA and SDS were dissolved in the aqueous phase. The reaction mixture was immersed in a water/ice bath, followed by a purging with nitrogen for 30 min to remove any redundant air, and then a predefined amount of KPS was added (Table 1). The reaction chamber was immersed in a 50 °C water bath for 8 h, after which, with the use of excess acetone, copolymers were precipitated. The precipitated product was again dissolved in the water, then precipitated by using the excess acetone and dried in a vacuum oven at a temperature of 60 °C for 24 h. The purified and dried products were then subjected to the various analyses. It should be mentioned that to obtain individual and overall conversion of the monomers, and compare it with the gravimetrically obtained conversion, in the case of experiment AB-4, a portion of the final reaction mixture (Table 1) was taken, and a small amount of hydroquinone as an inhibitor was added and dried without any purification and subjected to ^{1}H-NMR analysis.

Characterization

FTIR spectroscopy was used for characterization of the structure and functional groups of the synthesized copolymers. FTIR spectra were recorded over a wavelength range of 400–4000 cm^{-1} at ambient temperature using a PerkinElmer Spectrum (version 10.03.06) instrument. The samples were prepared in tablet form obtained from a mixture of KBr powder and milled synthesized products. For NMR spectroscopy measurement, a Bruker 400 MHz spectrophotometer was used. For the study the copolymer composition and structure, ^{1}H-NMR and ^{13}C-NMR spectra were considered. A powdered sample (about 3 wt%) was dissolved in D_2O and the obtained solution was used for analysis. For sample AB-1 (samples labeled by experiment; Table 1), deuterated acetone/D_2O (1/4 vol/vol) was used for preparing the NMR solution.

A Ubbelohde viscometer with a capillary diameter of 0.6 mm was used for measurement of intrinsic viscosity at 25 °C, from which the molecular weight of the products was estimated. Intrinsic viscosity ([η]) and Huggins equation coefficient (K_H) can be calculated from experimental data of polymeric solutions at various concentrations using Eq. (1) [16]. Considering the lower concentrations of BA in comparison to the concentration of AM in the initial feed, and thereby in the copolymer chain, the Mark-Houwink equation (Eq. (2)) proposed for PAM can be used to calculate the molecular weight of copolymers from intrinsic viscosity data [1–4, 15–17]. For intrinsic viscosity measurements, a 0.1 M solution of NaCl at 25 °C was used [1]. There is no Mark–Houwink relationship for the AM/AMPS copolymer from which to determine the molecular weight of the AM/AMPS/BA terpolymer (sample AB-5) in the 0.1 M solution of NaCl at 25 °C [36].

$$\frac{\eta_{sp}}{c} = [\eta] + K_H[\eta]^2 c \quad (1)$$

$$[\eta] = 9.33 \times 10^{-3} M_W{}^{0.75} \quad (2)$$

where η_{sp} is specific viscosity, [η] is the interstice viscosity in ml/g, c indicates the copolymer concentration in g/ml, K_H is the coefficient of the Huggins equation in g/ml, and M_W is the viscosity (or almost equivalent weight)-average molecular weight in g/mol.

To investigate the associative behavior of BA hydrophobic groups and to calculate the hydrodynamic radii (R_h) of copolymer chains in the aqueous medium, a DLS system (Zetasizer Nano S90) was used. Dilute aqueous solutions (with concentrations lower than 0.1 wt%) were prepared and centrifuged at 14,000 rpm to remove impurities. The tests were carried out at ambient temperature (25 °C) and at a wavelength of 633 nm,

Table 1 Details of reactions considered in the synthesis of samples via heterogeneous and micellar copolymerization methods[a]

Experiment no.	AM		BA		AMPS		SDS (g)	Conversion (%)
	g	%mol	g	%mol	g	%mol		
A-1[b]	1.2	100	–	–	–	–	1.2	78
AB-1	1.056	93	0.144	7	–	–	1.2	73
AB-2	1.056	93	0.144	7	–	–	0	82
AB-3	1.0	90	0.200	10	–	–	1.2	75
AB-4	1.0	95	0.100	5	–	–	1.2	77
AB-5	0.735	79.5	0.144	8.6	0.321	11.9	1.2	72
AB-6	1.056	93	0.144	7	–	–	0.6	70

[a] KPS=0.05 %wt relative to the aqueous phase, total monomer=3 %wt relative to the aqueous phase

[b] Basic reaction in the presence of SDS as emulsifier

where viscosity of the solution and the refractive index of the solvent and solution were used in the calculations. The DLS technique can be used to determine the polymer chain diffusion coefficient (D), from which the hydrodynamic radii of polymer coils can be calculated by considering the Stokes–Einstein equation (Eq. (3)) [37].

$$D = \frac{kT}{6\pi\eta R_h} \tag{3}$$

Here, k is the Boltzmann constant, T is temperature in Kelvin, η is the solution viscosity in cP, and R_h indicates the hydrodynamic radii of the polymer chains in nm.

Results and discussion

Heterogeneous and micellar copolymerization were used for the synthesis of the AM/BA copolymers and AM/AMPS/BA terpolymer (Fig. 1). In the heterogeneous copolymerization, AM along with the water-soluble portion of BA and were copolymerized in the aqueous phase. While there is no report on the homogeneous copolymerization of AM and BA in water as a solvent, reactivity ratios of AM (r_{AM}) and BA (r_{BA}) in a free radical solution (DMF) copolymerization were reported to be r_{AM}=0.69 and r_{BA}=1.24 [32]. Thus, the BA sequence length can be calculated using Eq. (4) [38].

$$\overline{n}_{BA} = r_{BA}\frac{f_{BA}^{o,sat}}{f_{AM}^{0}} + 1 \tag{4}$$

where ${f_{BA}}^{0,sat}$ indicates the water-soluble portion of BA as its mole fraction in the aqueous phase. The water solubility of BA was reported to be 0.18 wt% in 50 °C [39], from which ${f_{BA}}^{0,sat}$ was calculated by considering the reaction mixture in the present work to be 0.027. ${f_{AM}}^{0}$ indicates the initial mole fraction of AM in the aqueous phase. $\overline{n}_{BA}$ is the instantaneous sequence length of the BA incorporated into the copolymer, for which a value of 1.04 was obtained.

Based on the reactivity ratios and BA sequence length, a random distribution of BA in the main chain can be concluded, and a microstructure form of $[(AM)_n\text{-co-}(BA)_m]_p$ can be expected for the copolymers synthesized via the heterogeneous method (Fig. 2). It should be mentioned that in heterogeneous polymerization, only the water-soluble portion of BA can be expected to participate in the copolymerization reaction, and the remaining portion aggregates in the aqueous phase as a monomer droplet (Fig. 1). With the entry of the growing radicals into the BA monomer droplets, a BA-rich water-insoluble copolymer is expected to be formed, resulting in an unclear stirred solution. However, the reaction mixture in the micellar copolymerization remained clear during polymerization, suggesting that the entrance of growing radicals into the large monomer droplets can be neglected.

In micellar copolymerization, similar to the process that occurs with heterogeneous polymerization, the water-soluble portion of BA in the aqueous phase forms copolymer chains with a random distribution as $[(AM)_n\text{-co-}(BA)_m]_x$ (Fig. 2), and the remaining portion of the BA dissolves in the SDS micelle. In other words, the micelles provide favorable sites for the aggregation of BA molecules, where upon the entrance of growing macro-radicals, small blocks of BA can be incorporated into the hydrophilic main chain. Thus, in micellar copolymerization, both random and multi-block distributions can be observed for BA [2, 5] (Fig. 1). A structure form of $[(AM)_n\text{-co-}(BA)_m]_x\text{-b-}(BA)_y]_z$ can then be realized for the obtained copolymers (Figs. 1 and 2).

Structural characterization of the copolymers and terpolymer

For characterization of the polymers, FTIR spectroscopy was used, and spectra recorded for the AM/BA copolymer (AB-1) and the AM/AMPS/BA terpolymer (AB-5) are shown in Fig. 3. A strong absorption peak at wavelength of 1650 cm^{-1} can be observed in the spectrum of the AB-1 sample corresponding to the stretching vibration of the carbonyl

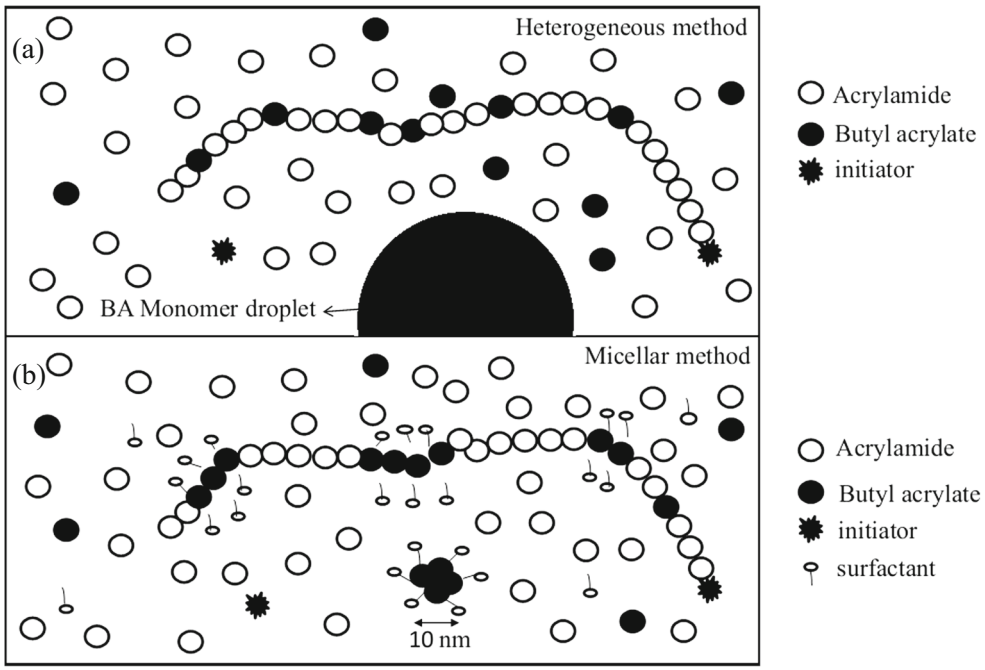

Fig. 1 The different mechanisms of copolymerization of AM/BA in the absence of surfactant (heterogeneous copolymerization) (**a**) and in the presence of surfactant (micellar copolymerization) (**b**)

group in the AM and BA. The observed peaks at wavelengths of 2870 and 2930 cm^{-1} account for stretching vibrations of the -CH bond present in the AM and BA. The stretching vibration of the amide bond (-NH) that emerged around a wavelength of 3430 cm^{-1} and the peak around a wavelength of 1451 cm^{-1} are related to the bending vibration of the $-CH_3$ bond of BA [34, 40, 41]. A similar spectrum was found for all other AM/BA copolymer samples. In the spectrum of terpolymer AB-5, a strong absorption band at wavelengths of 1040 and 1185 cm^{-1} can be observed due to the stretching vibration of the -S=O bond in the AMPS structure. In addition, a strong absorption peak at a wavelength of 1654 cm^{-1} corresponds to the stretching vibration of the -C=O bond in the AM, BA and AMPS structures (Fig. 3) [9, 40].

To determine the structure of the synthesized copolymers, the ^{1}H-NMR and ^{13}C-NMR spectra were also recorded. The structure of the synthesized homo-, co- and terpolymers, together with the assignment of all peaks to the corresponding protons, is illustrated in Fig. 4. For the AM/BA copolymers in Figs. 4.2 and 4.3, the observed broad peaks at chemical shifts of around 1.2–2 and 2–2.4 ppm can be related to the $-CH_2$ and -CH protons of both AM and BA in the main chain. The methyl ($-CH_3$) peak in BA was observed at around 0.8 ppm. In addition, the peaks of the two $-CH_2CH_2-CH_3$ of two methylene protons of BA at a chemical shift range of about 1.4–1.7 ppm overlapped with those of AM and BA protons in the main chain. Due to rapid proton exchange with D_2O, the expected broad peak of the amide group was no longer discernible; however, two weak peaks emerged around 6.5–7.8 ppm [28]. The chemical shift at about 4 ppm can be attributed to the methylene protons of $-OCH_2-$ present in the BA. The strong peak at a chemical shift of 4.7 ppm was assigned to the water (HOD). In the case of copolymer sample AB-1, where D_2O/acetone-d_6 were used as solvent, the quintet peak at 2.11 ppm

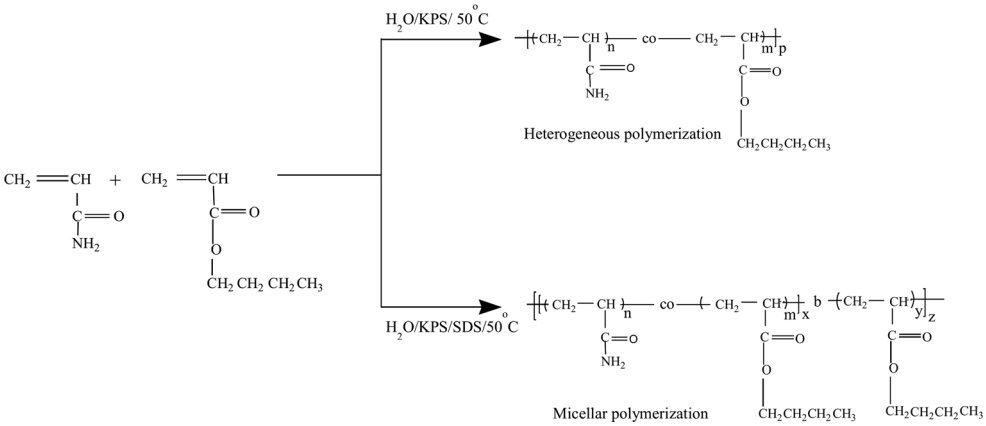

Fig. 2 Schematic representation of the copolymerization of AM and BA in water as solvent under various conditions and possible microstructures of the produced copolymers

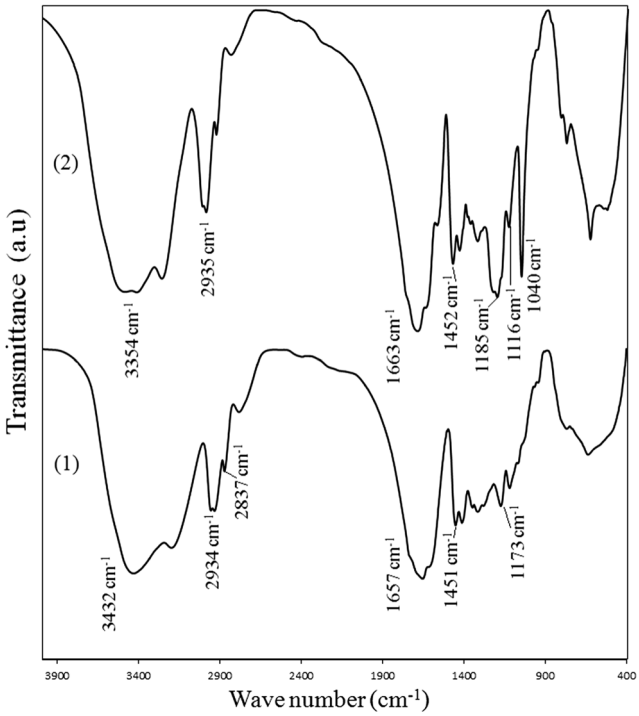

Fig. 3 FTIR spectra recorded for samples AB-1 (*1*) and AB-5 (*2*)

was assigned to the proton of the deuterated acetone (-CD_2H) [41, 42]. Similar spectra were found for all other AM/BA copolymer samples.

In the terpolymer sample AB-5, broad peaks appeared around a chemical shift of 1.2–2 and 2–2.4 ppm, which are related to the -CH_2- and -CH- protons of the main chain of the AM/AMPS/BA terpolymer (Fig. 4.4). In addition, the peaks of the -$\underline{CH_2}\underline{CH_2}$-$CH_3$ methylene protons in BA and methyl protons in AMPS overlapped with the peaks of protons in the main chain of the terpolymer. The broad peak in a chemical shift of 3.1–4 ppm was assigned to the -CH_2- methylene group in the side chain of AMPS.

Due to favorable water solubility, sample AB-2 synthesized using the heterogeneous method was used in the ^{13}C-NMR test. The ^{13}C-NMR and DEPT-135 spectra of the heterogeneous sample, together with the assignment of peaks to the corresponding carbons, are shown in Fig. 5, where peaks appearing at around 180 and 177 ppm corresponded to the carbonyl groups of AM and BA, respectively. The chemical shift values at 10, 18 and 30 ppm correlated to the carbons in -$CH_2CH_2CH_3$ of BA respectively. The carbon in the -OCH_2- group of BA was observed in a chemical shift of 68 ppm. For carbons of -CH_2- and -CH- in the copolymer main chain, broad peaks were found around 35 and 40 ppm, respectively. To validate the ^{13}C-NMR spectra, the DEPT-135 spectra were provided, in which the peaks for carbon of the first and third types (-CH- and CH_3, respectively) were upward-pointing, while peaks for the second type (-CH_2-) were downward-pointing (Fig. 5).

Determination of co- and terpolymer composition

The ^{1}H-NMR technique is a reliable method for determining the composition of copolymers, provided that the mole fraction of the comonomers in the copolymer is considerable (above 1 wt% similar to butyl acrylate) or a methyl group with three protons is available in the hydrophobic group [5–8]. The mole fraction of BA in a copolymer can be calculated by the intensity of the BA and AM proton peaks using ^{1}H-NMR spectra. Thus, by considering the assignment of the peaks to their corresponding protons (as illustrated in Fig. 4) and the integral of the peaks, it is possible to calculate the mole fraction of BA in the AM/BA copolymer ($F_{BA,copolymer}$) and the mole fractions of BA ($F_{BA,terpolymer}$) and AMPS ($F_{AMPS,terpolymer}$) in the terpolymer chain (sample AB-5) using Eqs. (5)–(7), respectively.

$$F_{BA,copolymer} = \frac{2I_a}{2I_a + 3\left(I_{b,c,e,f} - 2I_a\right)} \tag{5}$$

$$F_{BA,terpolymer} = \frac{I_a}{3I_{g,h,n}} \tag{6}$$

$$F_{AMPS,terpolymer} = \frac{I_q}{2I_{g,h,n}} \tag{7}$$

where I_i is the integral of proton(s) i, and $F_{i,copolymer}$ and $F_{i,terpolymer}$ indicate the mole fractions of comonomer i in the copolymer and terpolymer chains, respectively. The mole fractions of the monomers in the initial feed (f_i^0) and in the produced copolymer (F_i) are summarized in Table 2. The results show that the mole fraction of BA in sample AB-1 is higher than that in the sample AB-2, since as a consequence of polymerization in micelles, BA is incorporated more rapidly into the AB-1 structure than the AB-2 structure. The BA mole fraction in sample AB-4 was decreased as a result of a decrease in the amount of BA in the initial feed. A decrease in the mole fraction of BA in the terpolymer was also observed, suggesting that incorporation of BA into the main chain can be affected by the presence of AMPS in the feed (Table 2).

The mole fraction of BA in the AM/BA copolymer synthesized by free radical heterogeneous copolymerization was calculated using the Mayo–Lewis relationship (Eq. (8)) [42] as

$$F_{BA} = \frac{r_{BA}f_{BA}^2 + f_{AM}f_{BA}}{r_{BA}f_{BA}^2 + 2f_{AM}f_{BA} + r_{AM}f_{AM}^2} \tag{8}$$

where f_i is the mole fraction of the comonomer i in the initial feed, F_i indicates the instantaneous mole fraction of comonomer i incorporated into the copolymer, and r_i is the reactivity ratio of comonomer i.

The calculation results are presented in Table 3. For a theoretical case with BA saturation in the aqueous phase, one can

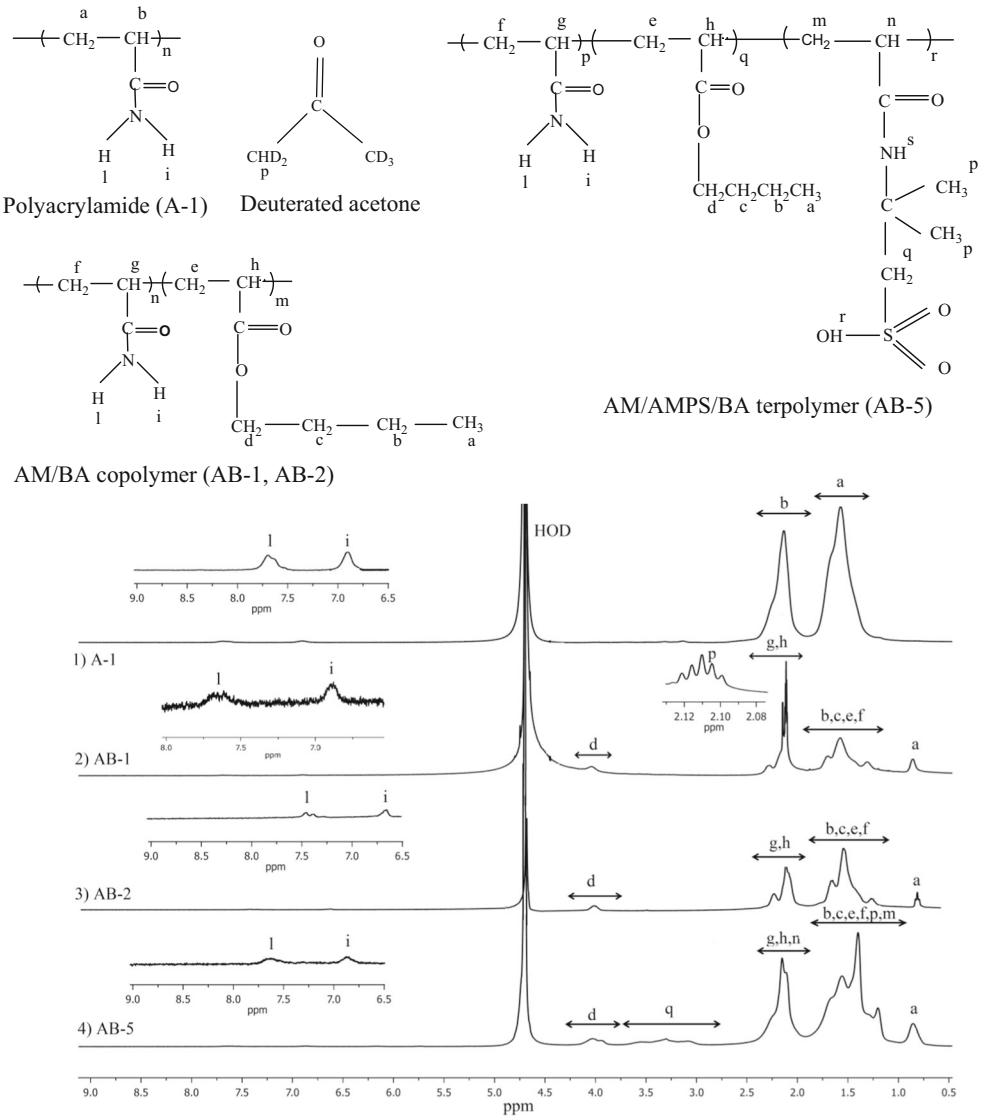

Fig. 4 ^{1}H-NMR spectra of AM homopolymer (A-1), AM/BA copolymer (AB-1 and AB-2) and AM/AMPS/BA terpolymer (AB-5) in D_2O solvent, along with their corresponding structure and assignment of peaks to corresponding protons

assume that BA is added to the reaction mixture only in an amount exactly equal to its water solubility (i.e., $f_{BA}^{o,sat}$=0.027) (Table 3). The system can then be considered to proceed via homogeneous copolymerization in the water. This situation results in the theoretical value of F_{BA}^{sat}=0.038. On the other hand, by assuming that all BA present in experiment AB-2 can be dissolved in the aqueous phase, one can then expect from Eq. (8) that $F_{BA,theor.}$ should be equal to 0.097 (Table 3). However, experimental F_{BA} for sample AB-2 obtained from corresponding ^{1}H-NMR spectrum was found to be 0.066 (Table 3). Experimental F_{BA} is higher than the theoretical one in the saturation case (i.e., F_{BA}^{sat}=0.038), while it is lower than the theoretical one (i.e., $F_{BA,theor.}$=0.097), indicating that copolymerization of BA and AM proceed in the aqueous phase only in the presence of insoluble BA droplets, where monomer droplets act only as a BA reservoir (Fig. 1).

Evaluation of the reaction conversion

A gravimetric procedure based on the difference between the initial monomer weight and the obtained polymer weight was used to calculate the reaction conversion, which was shown to be in a range of 70–80 %, as listed in Table 1. Because polymer loss may have occurred during the washing and precipitation steps, the ^{1}H-NMR technique was employed to calculate the accurate conversion value and compare it with the value obtained using the gravimetric method. The ^{1}H-NMR spectrum recorded for the reaction mixture dried without any purification of sample AB-4, including unreacted AM monomer, surfactant and the obtained copolymer, is shown in Fig. 6. The unreacted BA, along with the water, was evaporated during drying of the sample. Peaks were assigned to the corresponding protons for the synthesized copolymers. A peak appearing at around 6.65 ppm was assigned to the

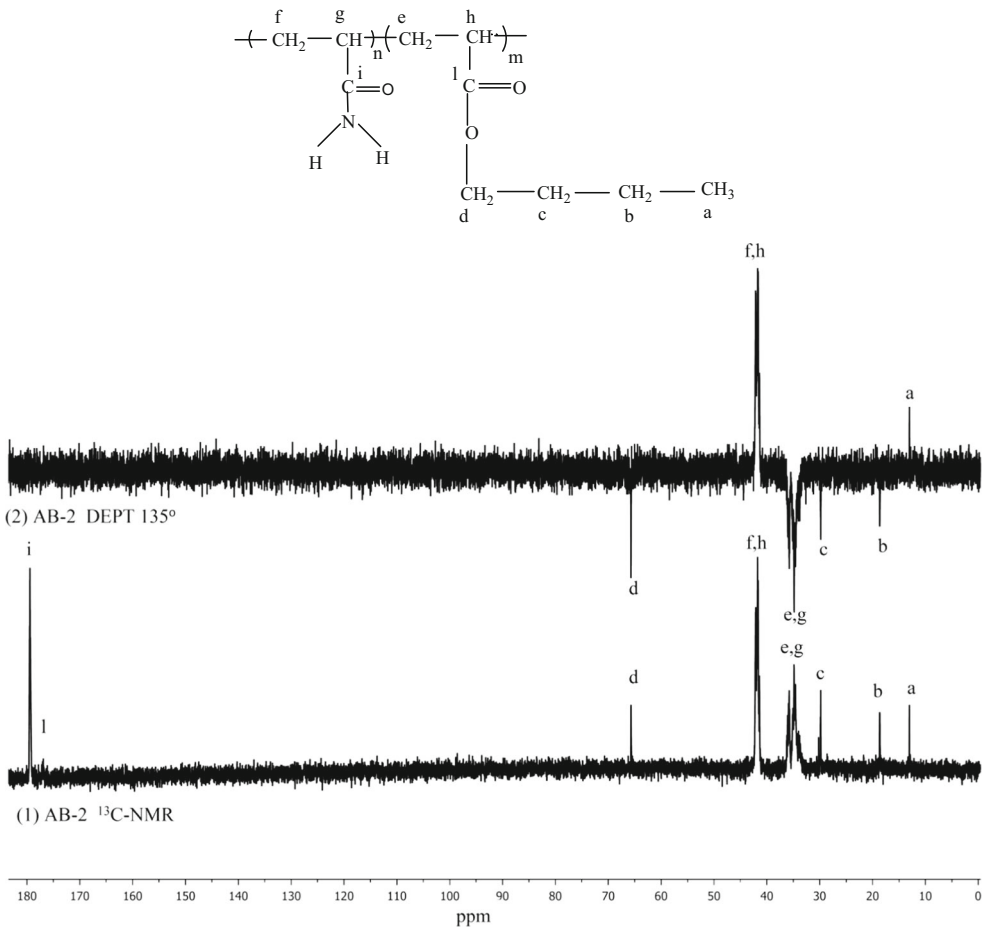

Fig. 5 DEPT-135 (*top*) and proton-decoupled ^{13}C-NMR (*bottom*) spectra recorded for sample AB-2 in D_2O solvent, along with assignment of peaks to the corresponding carbons

aromatic protons of the hydroquinone inhibitor. The mole fraction of BA in the initial feed was 0.05. The intensities equal to one proton from unreacted AM monomer ($I_{AM,unreacted}$), SDS (I_{SDS}), AM ($I_{AM,copolymer}$) and BA ($I_{BA,copolymer}$) incorporated into the copolymer can be calculated from the ^{1}H-NMR spectrum (Fig. 6) using Eqs. (9)–(12), respectively.

$$I_{AM,unreacted} = I_{e_2} \tag{9}$$

$$I_{SDS} = \frac{I_a}{2} \tag{10}$$

$$I_{AM,copolymer} = \frac{\left[\left(I_{h_1,h_2,g_2,g_3,b} + I_c\right) - \left(10I_a + 3I_{g_4}\right)\right]}{2} \tag{11}$$

Table 2 Mole fraction of monomers in the initial feed and the produced copolymer

Experiment no.	f^0_{BA}	f^0_{AMPS}	F_{BA}	F_{AMPS}
AB-1	0.070	–	0.084	–
AB-2	0.070	–	0.066	–
AB-4	0.050	–	0.037	–
AB-5	0.086	0.119	0.061	0.12

$$I_{BA,copolymer} = \frac{I_{g_4}}{2} \tag{12}$$

As mentioned previously, during the drying process, the unreacted BA monomer was removed from the reaction mixture, the amount of which can now be calculated using Eq. (13).

$$f^0_{BA} = \frac{I_{BA,copolymer} + y}{I_{BA,copolymer} + y + I_{AM,copolymer} + I_{AM,unreacted}} \tag{13}$$

where y represents the intensity value of one proton from the unreacted BA.

Table 3 Mole fraction of BA in the feed and in the copolymer for sample AB-2 synthesized via heterogeneous polymerization

f^0_{BA}	F_{BA}	
	Theoretical[a]	^{1}H-NMR
0.070	0.097	0.066
0.027[b]	0.038	–

[a] Theoretical values were calculated via Eq. (8) using f^0_{BA} values given in this table

[b] Saturated mole fraction of BA in the aqueous phase ($f^{0,sat}_{BA}$) calculated from the water solubility of BA (0.18 wt%) [38]

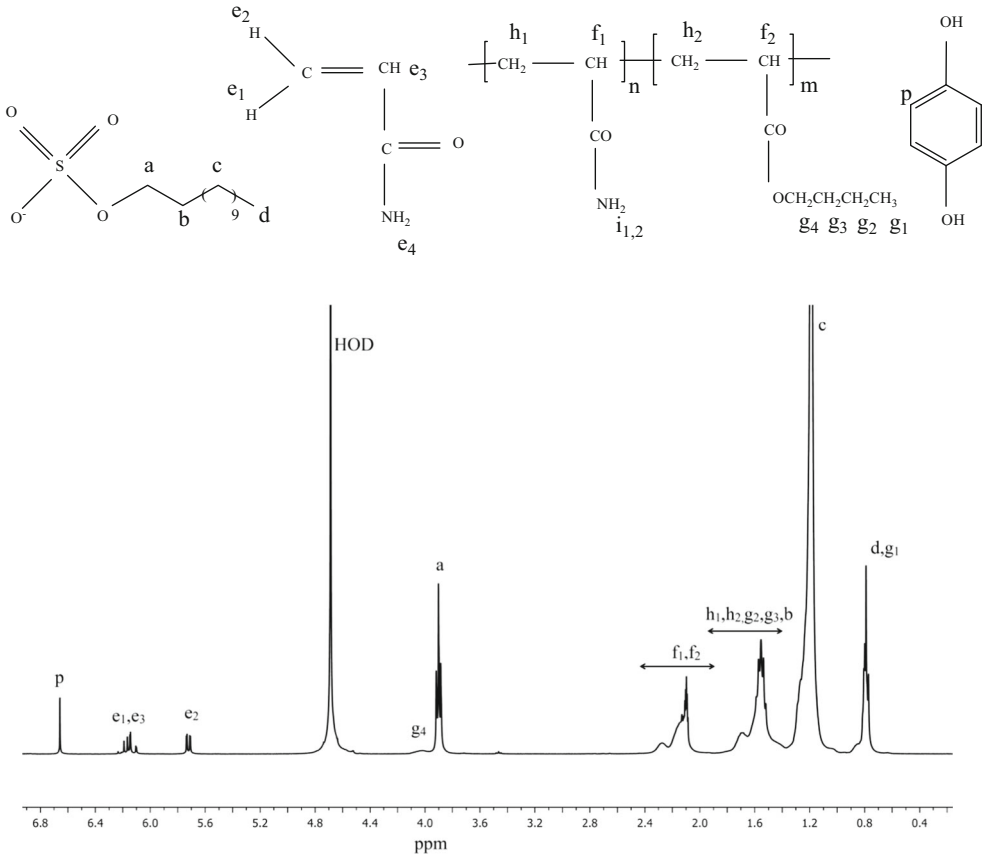

Fig. 6 ^{1}H-NMR spectrum recorded for the reaction mixture of sample AB-4, after vacuum drying with no purification, in the D_2O solvent

Individual molar conversions of AM (x_{AM}) and BA (x_{BA}), calculated using Eqs. (14) and (15), respectively, were determined as x_{AM}=0.931 and x_{BA}=0.625.

$$x_{BA} = \frac{I_{BA,copolymer}}{I_{BA,copolymer} + y} \tag{14}$$

$$x_{AM} = \frac{I_{AM,copolymer}}{I_{AM,copolymer} + I_{AM,unreacted}} \tag{15}$$

With the individual molar conversions at hand, the overall molar conversion of the monomers (x) was calculated using Eq. (16), reflecting a value of 0.916.

$$x = f^0_{BA} \times x_{BA} + f^0_{AM} \times x_{AM} \tag{16}$$

The overall mass conversion of the monomers (w) can be calculated from the x value via Eq. (17), provided that the value of F is known.

$$x = \frac{w(1+F)(1+f^o\mu)}{(1+f^o)(1+F\mu)} \tag{17}$$

where $f^o = f^0_{BA}/f^0_{AM}$, $F = F_{BA}/F_{AM}$ and $\mu = M_{BA}/M_{AM}$, in which M_i indicates the molecular weight of comonomer i.

The mole fraction of BA (F_{BA}) and AM (F_{AM}) incorporated into the copolymer chains can be obtained using Eqs. (18) and (19), respectively.

$$F_{BA} = \frac{I_{BA,copolymer}}{I_{AM,copolymer} + I_{.BA,copolymer}} \tag{18}$$

$$F_{AM} = \frac{I_{H,AM(polymer)}}{I_{H,AM(polymer)} + I_{H,BA(polymer)}} \tag{19}$$

For experiment AB-4, values of F_{BA}=0.0335 and F_{AM}=0.9665 were obtained from the corresponding ^{1}H-NMR spectrum (Fig. 6). Good agreement was observed between this spectrum and that already recorded for purified sample AB-4 (F_{BA}=0.037, Table 2).

An overall mass conversion value of w=0.904 was obtained from the ^{1}H-NMR spectrum in Fig. 6 using Eq. (17), which is higher than that obtained with the gravimetric procedure (w=0.77, as listed in Table 1),reflecting the polymer losses during the washing and precipitation steps.

Determination of the molecular weight

In the present work, the intrinsic viscosity of the synthesized AM/BA copolymers was calculated using Eq. (2). Table 4 shows the intrinsic viscosity, Huggins equation coefficient and molecular weight of the samples. As samples AB-3 and AB-6 were insoluble in water, their molecular weight cannot be calculated. In the case of the AM/BA/AMPS polyelectrolyte, due to the substantial incorporation of AMPS into the

Table 4 Results of intrinsic viscosity, Huggins equation coefficient and molecular weight obtained for various AM/BA copolymers in 0.1 M NaCl aqueous solution at a temperature of 25 °C

Experiment no.	[η] (mLg^{-1})	K_H	$M_w \times 10^6$ ($gmol^{-1}$)
A-1	199.00	0.87	0.589
AB-1	106.46	2.12	0.256
AB-2	404.31	0.31	1.516
AB-4	280.41	0.58	0.931

terpolymer chains, and its significant influence on terpolymerization evolution, Eq. (2) cannot be used to estimate its molecular weight.

It is clear from the results presented in Table 4 that, compared to the other samples, sample AB-2 possesses the highest molecular weight (1.516×10^6 g/mol). The higher molecular weight of the copolymer synthesized using the heterogeneous method, i.e., sample AB-2, can be attributed to the lower contribution of chain transfer reactions in the absence of chain transfer agents (such as SDS) [2]. A low molecular weight of 2.56×10^5 g/mol was observed for sample AB-1 in the presence of SDS, which can act as a chain transfer agent [2]. There is no molecular weight data for sample AB-5 (Table 4). The molecular weight of micellar sample AB-4, even in the presence of SDS, was relatively high, at 9.31×10^5 g/mol. The reduced viscosity of the AB-5 sample was improved by adding NaCl.

In comparison to the copolymer samples, the micellar-synthesized PAM homopolymer (sample A-1) revealed lower molecular weight values, which can be explained simply by the transfer reactions that occurred in the presence of SDS. Using Eq. (1), the intrinsic viscosity and Huggins equation coefficient were calculated, and a reciprocal relationship was realized for these two parameters (Table 4). The highest and lowest intrinsic viscosities were obtained for samples AB-2 and AB-1, respectively, which is directly related to their molecular weight.

Relationship between the microstructure and water solubility of copolymers

The BA block length can be calculated in terms of the number of hydrophobic monomers per micelle (N_H) as presented by Eq. (20) [27–29].

$$N_H = \frac{C_{HM}}{(C_S - CMC)/N_{agg}} \approx \frac{C_{HM}}{C_S} \times N_{agg} = \frac{N_{agg}}{SMR} \quad \text{where} \quad SMR = \frac{C_S}{C_{HM}} \tag{20}$$

where C_{HM} is the molar concentration of hydrophobic monomers, C_S is the molar concentration of the surfactant, CMC is the critical micelle concentration of the surfactant, and N_{agg} is the micelle aggregate number, which is equal to 60 for SDS at 50 °C [22]. A value of 9.2 mM at 50 °C has been reported for the CMC of SDS [22]. One might simply neglect the CMC in comparison to C_S, as C_S is very high. The hydrophobic block length (N_H) can be determined using N_{agg} and surfactant-to-monomer ratio (i.e., SMR) [1–6]. An increase in N_H or a decrease in SMR would result in water-insoluble HMPAM copolymers; therefore, the HMPAM must be optimized in a way that desirable rheological property and solubility could be obtained [2].

To calculate BA block length (N_H(, Eq. (20) was modified as Eq. (21) to account for the considerable concentration of BA in the aqueous phase.

$$N_H = \frac{C_{HM} - C_{HM}^{aq}}{(C_s - CMC)/N_{agg}} \quad \text{where} \quad SMR = \frac{C_s}{C_{HM} - C_{HM}^{aq}} \tag{21}$$

where C_{HM}^{aq} is the molar concentration of the water-soluble portion of BA. The calculated SMR and N_H data, along with the water solubility data, are summarized in Table 5.

It is clear from the results given in Table 5 that, in micellar copolymerization, the hydrophobic block length increases as the BA content in the initial feed increases, resulting in the multi-block distribution of BA in the main chain. The solubility of the polymer decreases as the N_H value increases or equivalent SMR value decreases. A microstructure-related interpretation can be applied for the water solubility of polymers. In other words, the water solubility of the multi-block copolymers synthesized via micellar copolymerization decreases as the hydrophobic block length increases. Compared to that for sample AB-1, the BA content in the initial feed for sample AB-3 was increased by 10 wt%; hence, this sample was insoluble in the aqueous phase due to the increased hydrophobicity as a result of increased hydrophobic block length (Table 5). For sample AB-6, where the SDS content was decreased to half that in AB-1, the number of micelles decreased, and consequently, N_H increased significantly. Thus the BA block length increased suddenly, resulting in a water-insoluble polymer (AB-6) due to the formation of an intermolecular aggregation network of BA hydrophobic blocks.

Table 5 The main and effective parameters of the reaction evolution and properties of the prepared samples

Experiment no.	SMR	N_H	Method	Water solubility
A-1	–	–	Micellar	++[a]
AB-1	3.7	14.9	Micellar	+
AB-2	0	1	Heterogeneous	++
AB-3	2.6	20.7	Micellar	–
AB-4	5.3	10.3	Micellar	++
AB-5	3.7	14.9	Micellar	++
AB-6	1.8	33.8	Micellar	–

[a] Excellent solubility (++), good solubility (+), insoluble (–)

Table 6 Results of the estimation of microstructure-related parameters of the synthesized AM/BA copolymers

Experiment No.	F_{BA}	n_{av}	m_{av}	y_{av}	x_{av}
AB-1	0.0845	25.28	1	14.9	10.92
AB-2	0.0662	25.28	1	–	–
AB-4	0.0372	25.28	1	10.3	430.87

However, both samples AB-3 and AB-6 were dissolved in an aqueous solution containing SDS in a concentration higher than the CMC value. Hydrophobic side groups of BA can individually dissolve in SDS micelles. Therefore, the intermolecular aggregation network formed from the BA hydrophobic blocks disappears, increasing the water solubility of the copolymers. Relatively insoluble behavior was also observed for sample AB-1, for which some insoluble microscopic coagulation emerged. This can be attributed to the higher BA content incorporated into the copolymer (Table 2). Sample AB-2 was dissolved quickly in the water due to a random distribution of BA comonomer that occurred with the heterogeneous procedure. On the other hand, sample AB-4 was a perfect water-soluble polymer, indicating that a BA block length of about 10 had no negative effect on its solubility, and thus an optimal N_H value of 10 can be realized.

As mentioned previously, a random distribution of BA in the copolymer chain with a general microstructure of $[(AM)_n\text{-co-}(BA)_m]_p$ can be considered for a AM/BA copolymer synthesized via heterogeneous polymerization, while in micellar copolymerization, additional multi-block distribution off BA units in the copolymer chain with a general microstructure of $[(AM)_n\text{-co-}(BA)_m]_x\text{-b-}(BA)_y]_z$ can be proposed (Fig. 2). In the following section, efforts will be made to estimate microstructure-related average values of n (n_{av}), m (m_{av}), x (x_{av}) and y (y_{av}) indexes (Table 6).

The sequence length of BA in the aqueous phase-formed copolymer was calculated using Eq. (4) to be 1.04. Thus, the value of index m can be considered a unit. Similarly, the instantaneous sequence length of AM ($\overline{n}_{AM}$) or equivalent index n in the aqueous phase-formed copolymer was calculated using Eq. (22) to be 25.28.

$$\overline{n}_{AM} = r_{AM}\frac{f_{AM}^{\ 0}}{f_{BA}^{\ 0,sat}} + 1 \tag{22}$$

The value of index y corresponds to the BA block length in the copolymers synthesized by micellar copolymerization. This value can be considered equal to the value of N_H (Table 5). With the average values of indexes m, n and y at hand, the average value of index x can be calculated using Eq. (23) (Table 6). The value of $x\times(n+m)$ indicates the average length of the growing chain in the aqueous phase, after which it enters into the SDS micelle containing y number of BA. The radical chain then enters into the aqueous phase and grows in the presence of AM and BA present in the aqueous phase. This process repeats $z/2$ times on average during the micellar polymerization followed by the combined termination of two growing macro-radicals to form copolymers with a microstructure shown in Fig. 2.

$$F_{BA} = \frac{(x \times m) + y}{[x \times (n + m)] + y} \tag{23}$$

,where F_{BA} is the average mole fraction of BA incorporated into the copolymer chain; corresponding values for samples AB-1, AB-2 and AB-4 are provided in Table 2. The values of microstructure-related parameters, i.e., n, m, x and y, are summarized in Table 6.

By considering the water solubility of the copolymers, one can conclude that the ratio of x/y in the micellar system can serve as an indicator for the water solubility of the copolymers. The higher the ratio of x/y is, the higher the water solubility of the copolymer will be, as can be seen in the case of sample AB-4 in comparison with sample AB-1 (Tables 5 and 6). In other words, it seems from Tables 5 and 6 that an NH value higher than about 10, along with an x/y ratio lower than about 1, can limit the water solubility of the synthesized copolymers. A higher ratio of x/y would indicate that BA present in the micelle should incorporate into the copolymer main chain at a much lower rate and with a shorter sequence length than AM and BA present in the aqueous phase. Consequently, multi-block copolymers with shorter hydrophobic sequence

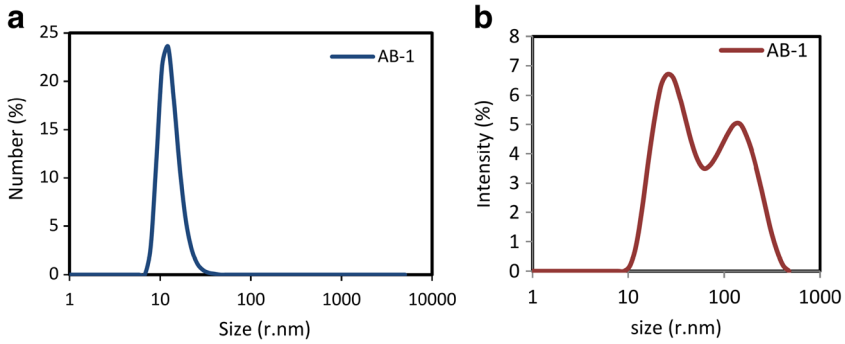

Fig. 7 DLS results obtained for sample AB-1: number distribution (**a**) and intensity distribution (**b**) of copolymer coils and BA intermolecular aggregations versus size

Table 7 Average hydrodynamic radii of polymer coils and intermolecular BA nano-aggregations obtained from DLS analysis of dilute aqueous solution at ambient temperature

Experiment No.	Number - average R_h (nm)	Intensity - average hydrophobic aggregates (nm)
AB-1	13.21	220
AB-2	5.65	100
AB-4	3.15	250
AB-5	35.54	200

length (i.e., shorter *y* or NH value) and larger *x* value would show the best water solubility

Calculation of R_h and analysis of hydrophobic nano-aggregation

The hydrodynamic radius of copolymer chain coils in dilute solutions shows the R_h of chains. Using the DLS technique, one would be able to analyze the hydrophobic aggregation of the HMPAMs. The intensity and number distribution of coil size for each sample was obtained using the DLS technique, as illustrated in Fig. 7 for sample AB-1. Similar curves were observed for other samples. The average R_h of the polymer coils was calculated using number distribution data, and the obtained values are summarized in Table 7.

It seems from Table 7 that higher hydrophobicity of the copolymers leads to a higher R_h value. The increase in hydrophobicity and hydrophobic aggregation of BA units results in the swelling of copolymer chains, and this behavior would be manifold in a multi-block polymer. The terpolymer AB-5 is a polyelectrolyte, for which rapid swelling of the chains occurs in an aqueous phase as a result of anionic charge repulsion, resulting in the higher R_h (Table 7).

Due to the presence of hydrophobic BA groups, aggregations with a size larger than that of R_h can be seen in the intensity-based size distribution diagrams (Fig. 7b). However, in comparison to that in the polymeric coils, the number of hydrophobic BA aggregations observed in the number distribution diagrams are very small and almost negligible. The average size of the hydrophobic intermolecular aggregations of BA falls within a range of 100–250 nm, as shown in Table 7. As BA aggregation in micellar copolymerization consists of random and multi-block portions, the R_h of BA aggregations in samples synthesized using the micellar technique is larger than that occurring in heterogeneous copolymerization.

Conclusions

Random and multi-block co- and terpolymers of AM/BA and AM/BA/AMPS as HMPAMs were successfully synthesized for the first time using heterogeneous and micellar methods. (Micro)structural characteristics including molecular weight, copolymer composition, hydrophilic AM and hydrophobic BA sequence lengths, and hydrophobic nano-aggregations were investigated using intrinsic viscosity measurement, ^{1}H-NMR and theoretical calculations, along with ^{1}H-NMR experimental data and DLS techniques, respectively. The highest molecular weight, 1.516×10^6 g/mol, was observed for the heterogeneous method, where no chain transfer agent (here SDS) was present in the reaction mixture. Monomer sequence lengths of approximately 1 and 25 were obtained for BA and AM, respectively, in heterogeneous polymerization, which corresponds to a random distribution of BA in the copolymer structure. In micellar copolymerization, BA aggregates in the micelles and small multi-blocks of BA were formed due to the entrance of growing radicals into micelles. The calculated length of BA blocks (N_H) varied, within a range of approximately 10–34. Water solubility evaluation of the synthesized samples demonstrated differences between the multi-block and random microstructures. Results obtained from water solubility and microstructure investigation of the polymers showed that a value of N_H higher than approximately 10, along with a microstructure-related parameter of the x/y ratio lower than approximately 1, can limit the water solubility of the BA/AM copolymers The overall mass conversion of monomers for sample AB-4 obtained using gravimetric and ^{1}H-NMR techniques was 0.77 and 0.90, respectively, indicating that polymer loss occurred during the washing and precipitation steps with the gravimetric method. The results of the R_h of polymer coils and hydrophobic intermolecular aggregations obtained by DLS measurements indicated that nano-aggregation of hydrophobic groups can be found in dilute polymeric solutions. The average R_h of polymer coils and average radii of BA hydrophobic group aggregations were found to be in a range of 3.15–35.54 and 100–250 nm, respectively. This study revealed that, with microstructure-related parameters at hand, a reasonable microstructure–water solubility relationship can be established for AM/BA copolymers synthesized using heterogeneous and micellar methods.

References

1. Hill A, Candau F, Selb J (1993) Macromolecules 26:4521–4532
2. Candau F, Selb J (1999) Adv Colloid Interf Sci 79:149–172
3. Volpert E, Selb J, Candau F (1998) Polymer 39:1025–1033
4. Wevera DAZ, Picchionia F, Broekhuis AA (2011) Prog Polym Sci 36:1558–1628
5. Volpert E, Selb J, Candau F (1996) Macromolecules 29:1452–1463
6. McCormick CL, Middleton JC, Grady CE (1992) Polymer 33: 4184–4190
7. Kathmann EE, White LA, McCormick CL (1997) Macromolecules 30:5297–5304

8. Noda T, Hashidzume A, Morishima Y (2001) Macromolecules 34: 1308–1317
9. Sabhapondit A, Borthakur A, Haque I (2003) J Appl Polym Sci 87: 1869–1878
10. Sabhapondit A, Borthakur A, Haque I (2003) Energy Fuels 17:683–688
11. McCormick CL, Nonaka T, Johnson CB (1988) Polymer 29:731–739
12. Dowling KC, Thomas JK (1990) Macromolecules 23:1059–1064
13. Lai N, Dong W, Ye Z, Dong J, Qin X, Chen W, Chen K (2013) J Appl Polym Sci 129:1888–1896
14. Zhong C, Zhang H, Feng L (2014) J Polym Res 21:604
15. Saadatabadi AR, Nourani M, Emadi MA (2010) Iran Polym J 19: 105–113
16. Ma J, Cui P, Zhao L, Huang R (2002) Eur Polym J 38:1627–1633
17. Gong LX, Zhang XF (2009) Express Polym Lett 12:778–787
18. Hassanajili S, Abdollahi E (2014) J Appl Polym Sci 131:39939
19. Lara-Ceniceros TE, Cadenas-Pliego G, Rivera-Vallejo CC, de León-Gómez RED, Coronado A, Jiménez-Regalado EJ (2014) J Polym Res 21:511
20. Hill A, Candau F, Selb J (1991) Colloid Interface Sci 84:61–65
21. Wang C, Li X, Li P (2012) J Polym Res 19:9933
22. Guo Y, Liang Y, Yang X, Feng R, Song R, Zhou J, Gao F (2014) J Appl Polym Sci 131:40633
23. Feng Y, Billon L, Grassl B, Khoukh A, François J (2002) Polymer 43:2055–2064
24. ValintJr PL, Bock J (1988) Macromolecules 21:175–179
25. Al-Sabagh AM, Kandile NG, El-Ghazawy RA, Naser El-Din M, El-sharaky EA (2013) Egypt J Pet 22:531–538
26. Wang C, Li X, Du B, Shen Y, Li P (2012) J Polym Res 20:42
27. Zhang Y-X, Da A-H, Butler G-B, Hogen-Esch T-E (1992) J Polym Sci Part A: Polym Chem 30:1383–1391
28. Zhang H, Xu K, Ai H, Chen D, Xv L, Chen M (2008) J Solut Chem 37:1137–1148
29. Zhuang D-Q, Da JCA, Zhang Y-X, Dieing R, Ma L, Haeussling L (2001) Polym Adv Technol 12:616–625
30. Schierholz K, Givehchi M, Fabre P, Nallet F, Papon E, Guerret O, Gnanou Y (2003) Macromolecules 36:5995–5999
31. Barton J, Capek I (2000) Macromolecules 33:5353–5357
32. Brar AS, Mukherjee M, Chatterjee SK (1998) Polym J 30:664–670
33. Yildiz U, Capek I, Berek D, Sarov Y, Rangelow IW (2007) Polym Int 56:364–370
34. Yin N, Chen K (2004) Polymer 45:3587–3594
35. Zhong C, Luo P, Ye Z, Chen H (2009) Polym Bull 62:79–89
36. Wu YM, Wang YP, Yu YQ, Xu J, Chen QF (2006) J Appl Polym Sci 102:2379–2385
37. Will S, Leipertz A (1995) Int J Thermophys 16:433–443
38. Dotson NA, Galvan R, Laurence RL, Tirrell M (1995) Polymerization process modeling. Wiley-VCH, London
39. Broze G (2011) Handbook of detergents. CRC Press, London
40. Liu J, Wang CX, Wu YM (2011) Iran Polym J 20:887–896
41. Pavia DL, Lampman GM, Kriz GS (2009) Introduction to spectroscopy, 4th edn. Cengage Learning, Boston
42. Abdollahi M, Alamdari P, Koolivand H, Ziaee F (2013) J Polym Res 20:239